Available online at www.sciencedirect.com
SCIENCE DIRECT®
Journal of Nuclear Materials 325 (2004) 202–209
journal of nuclear materials
www.elsevier.com/locate/jnucmat

Chemical diffusion in uranium dioxide – influence of defect interactions

P. Ruello [a], G. Chirlesan [a], G. Petot-Ervas [a,*], C. Petot [a], L. Desgranges [b]

[a] *Laboratoire Structures, Propriétés et Modélisation des Solides, CNRS-UMR 8580, Ecole Centrale Paris, Grande Voie des Vignes, 92295 Châtenay Malabry cedex, France*

[b] *Commissariat à l'Energie Atomique, DEC/SACCC/LEEC, Cadarache, 13104 Saint-Paul-lez-Durance, France*

Received 21 July 2003; accepted 3 December 2003

Abstract

The chemical diffusion coefficient of UO_{2+x} was determined from electrical conductivity measurements performed during transient state, for departure from stoichiometry in the range $0 < x < 0.17$ and for temperatures varying from 973 to 1673 K. It was found that $\widetilde{D}$ is a decreasing function of the departure from stoichiometry, while the oxygen diffusion coefficient reported in literature is an increasing function in the same range of departure from stoichiometry. For $x < 0.07$, this behavior was attributed to the presence of the singly ionized $(2{:}2{:}2)'$ Willis defects evidenced by electrical conductivity measurements. The enthalpy of formation of these clusters amounts to $\Delta H_f = -1.7 \pm 0.6$ eV. For $x \geqslant 0.07$, the decreasing function of $\widetilde{D}$ with x can be explained either by Willis defects α time ionized or more complex defect aggregates or via a dynamic exchange between mobile small defects and larger clusters or domains.

1. Introduction

Oxidation of uranium dioxide is an important mechanism for many industrial processes involving nuclear fuel such as reprocessing, sintering, severe accidents or interim storage. The kinetic of oxidation–reduction reactions is controlled by the prevailing point defects in the materials. Knowledge of both the thermodynamic properties and diffusion processes of these defects is thus important for understanding the oxidation of $UO_{2\pm x}$, but also for explaining a wide variety of solid state reactions, such as sintering or kinetic demixing [1–7], or for predicting the mass transport processes rate-controlled by the diffusion of the slower species and occurring during creep [2–4], for instance. Despite the extensive investigations devoted to this oxide for safety considerations, a number of points are still in need of clarification, such as the point defect structure and the mechanism of oxygen migration.

One can briefly recall that this oxide adopts the fluorite structure, in which the uranium cations form a face centred cubic lattice while the oxygen anions form a simple cubic lattice. This structure presents the ability to accommodate a very high concentration of defects on the oxygen sublattice. This property coupled to the facile valence change, $U^{4+} \Longleftrightarrow U^{5+}$, enables this ceramic to reach departure from stoichiometry up to at least $UO_{2.3}$. At the stoichiometric composition, the prevailing point defects are assumed to be oxygen Frenkel defects [1,4,8–12], while for departure from stoichiometry greater than 0.01, it is widely accepted that the increasing concentration of oxygen interstitials is stabilized by defect clusters of oxygen interstitials and oxygen vacancies suggested by Willis [9–13] and schematized by $(2O_i^{a'}\ 2O_i^{b'}\ 2V_O^{c\cdot\cdot})^{\alpha'}$ or also $(2{:}2{:}2)^{\alpha'}$. In order to understand the oxygen diffusion mechanism, a number of investigators have studied the temperature and defect concentration (x) dependence exhibited by the self-diffusion of oxygen D_O^* [1,4,10,11,14]. The available data show that D_O^*

* Corresponding author. Tel.: +33-1 41 13 13 23; fax: +33-1 41 13 14 37.
E-mail address: gpetot@spms.ecp.fr (G. Petot-Ervas).

0022-3115/$ - see front matter © 2003 Published by Elsevier B.V.
doi:10.1016/j.jnucmat.2003.12.007

increases with the departure from stoichiometry [14], with the occurrence of a maximum at about $x = 0.10$ proposed by Murch et al. [10,12]. On the other hand, it was found that the diffusion activation energy does not vary very much except near the stoichiometry composition ($x < 0.006$), where an increase of E_a is observed [14]. At the present time, oxygen diffusion is believed to occur mainly by vacancy motion in stoichiometric UO_2 and by oxygen interstitials, probably in clusters, in UO_{2+x} [8–12,14], but it is not clear how such defects move through the crystal. Do they move as discrete units or act as sources or sinks for highly mobile point defects? The difficulties encountered in the analysis of the transport processes on the oxygen sublattice lie in the fact that the oxygen diffusion coefficient is roughly proportional to the product of the defect concentration by their diffusion coefficient. Results concerning the chemical diffusion coefficient ($\widetilde{D}$) are also available [1,15–21]. These data are important to analyse the oxygen diffusion processes since $\widetilde{D}$ is related only to the movement of oxygen ions in presence of a thermodynamical potential gradient. This coefficient has been obtained by monitoring the weight or electrical conductivity change after reduction or oxidation reactions. According to the available data, it seems that the chemical diffusion coefficient values obtained from an oxidation experiment are lower than those corresponding to a reduction experiment. However, these results have been obtained by different authors and under not well-defined oxygen partial pressures. Since in $UO_{2\pm x}$ the oxygen content of the sample has a large effect on the experimental results, this leads to inherent difficulties in the interpretation of the results.

The purpose of this study is both to determine the chemical diffusion coefficient of $UO_{2\pm x}$ and to precise the defect structure, as a function of the defect concentration and for different temperatures. A model of the transport processes under non-equilibrium conditions is also suggested to analyse the influence of the departure from stoichiometry on the $\widetilde{D}$ values.

2. Experimental methods

2.1. Electrical conductivity measurements

The electrical conductivity measurements were performed by the four probe technique at 1.5 kHz frequency, using a double Kelvin bridge [22,23]. Parallelepipedic samples have been machined with a diamond saw from a single crystal grown by an arc fusion technique. The main impurities are reported in Table 1. The two opposite ends of the rectangular samples were wrapped with platinum foils to ensure an uniform repartition of the current lines through the sample. Platinum wires were used as electrical junctions.

Table 1
Prevailing impurities in the urania single crystal

Elements	Weight amount (ppm)
Fe	560
Mn	155
Ca	123
V, Pb	10
K, Mg, P, Al, Ti, Cr, Cu, Zn, Zr, Nb, W, Th	$\leqslant 6$

They are connected to the double Kelvin bridge with null detector provided by a lock-in amplifier. The conductivity was determined from the classical relation:

$$\sigma = \sigma_0 \exp(-\Delta H_\sigma / RT) = e\mu_d C_d = \frac{1}{R}\frac{l}{S}, \quad (1)$$

where R is the measured electrical resistance between the two internal electrical junctions separated by a length l, S the cross-section of the sample, μ_d the mobility of the electronic defects (electrons/e′ or holes/h·), C_d their concentration per cm^3 and ΔH_σ the enthalpy of conductivity, related to the enthalpy of mobility ΔH_m^d of the electronic defects and to the enthalpy of formation of the point defects ΔH_f (cf. Eq. (5)).

Measurements were carried out in different flowing gas mixtures (Ar/H_2, $Ar/H_2/CO_2$ or CO/CO_2) to check that the electrical conductivity results were not influenced by the surrounding atmosphere. The oxygen partial pressure was monitored near the sample using an yttria-stabilized zirconia cell. The gas mixtures were performed with a Brook mass flowmeter.

Thermal and chemical equilibrium of the sample was systematically checked by cycling the oxygen partial pressure, for each isotherm, and by measurements performed in increasing and decreasing the temperature, at a given P_{O_2}.

2.2. Electrical conductivity measurements in transient state – determination of $\widetilde{D}$

The chemical diffusion coefficient ($\widetilde{D}$) was determined by following the electrical conductivity changes [22,32] after subjecting the sample, initially equilibrated with the surrounding atmosphere, to a sudden change of one of the thermodynamical equilibrium parameters (P_{O_2} or T). The sample reacts with the surrounding atmosphere and the point defect concentration at the surface corresponds immediately to the new equilibrium conditions. Therefore, a defect concentration gradient is set up at the near surface of the sample. It develops progressively in the bulk and decreases then until the new equilibrium conditions are reached. The flux of defects which appears in a crystal under the influence of

a defect concentration gradient in the z direction may be written, according to the Fick's law as [2,3]:

$$J_d = -\widetilde{D}\left(\frac{dC_d}{dz}\right), \tag{2}$$

where $\widetilde{D}$ is the chemical diffusion coefficient.

The knowledge of $\widetilde{D}$ allows the determination of both the mean penetration (Δz) of the oxidation–reduction front after a time t ($\Delta z \approx \sqrt{\widetilde{D}t}$) and the time to reach the new equilibrium conditions.

According to the long time approximation [2,22,24,25], the electrical conductivity ($\sigma(t)$) during the approach to the new thermodynamical equilibrium of the sample is expressed by the following exponential form:

$$\frac{\sigma(t)-\sigma_\infty}{\sigma_0-\sigma_\infty} = \left(\frac{8}{\pi^2}\right)^3 \exp -\pi^2\left(\frac{1}{H^2}+\frac{1}{L^2}+\frac{1}{l^2}\right)\widetilde{D}t, \tag{3}$$

where H, L, l are the dimensions of the sample and σ_0 and σ_∞ the initial electrical conductivity, when the thermodynamical equilibrium conditions are changed, and the conductivity when the new equilibrium conditions are reached, respectively.

The chemical diffusion coefficient is determined from the representations $\log(\sigma(t)-\sigma_\infty) = f(t)$.

Remark 1. Experiments carried out with two different size samples ($5.0\times2.3\times2.5$ or $5.2\times5.8\times4.2$ mm^3) and using different gas mixtures (Ar/H_2, $Ar/H_2/CO_2$ or CO/CO_2 mixtures) for close P_{O_2} step have allowed us to check that the values of $\widetilde{D}$ were not influenced by surface oxygen exchange processes.

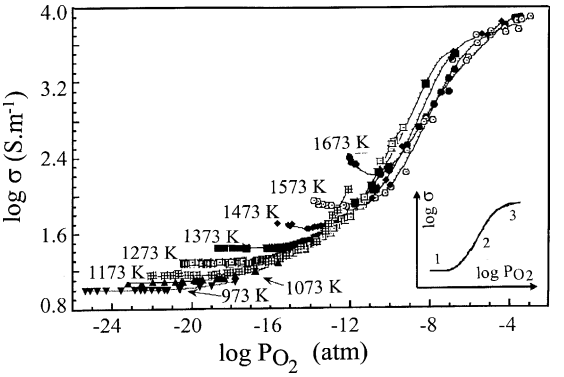

Fig. 1. Electrical conductivity of $UO_{2\pm x}$ as a function of the oxygen partial pressure. The inset visualizes three different regions as discussed in the text.

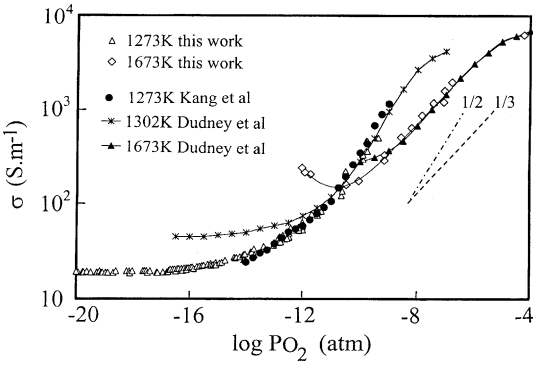

Fig. 2. Comparison of our electrical conductivity measurements with literature data [22].

3. Experimental results

3.1. Electrical conductivity results

Fig. 1 displays the electrical conductivity of $UO_{2\pm x}$ as a function of the oxygen partial pressure and for temperatures between 973 and 1673 K. According to thermogravimetric data [26–29], the measured conductivities concern the non-stoichiometry range between $x \sim 0$ and $x \sim 0.2$. The curves exhibit an 'S' shape in agreement with previous data [30,31] and can be divided into three regions (Fig. 2).

- *In the low P_{O_2} region (region 1)* and at $T \leqslant 1273$ K, the electrical conductivity isotherms show a plateau, the boundaries of which shift to higher P_{O_2} values with increasing temperature, while at $T > 1273$ K, the conductivity passes through a minimum. As we have shown in previous papers [23,32], region 1 corresponds to the near stoichiometric material. The electrical conductivity minima, coupled to Seebeck coefficient results, have allowed us to determine the relative partial molar free energy ($\Delta\bar{G}_{O_2}$) for the stoichiometric oxide, with a high accuracy [23–32].
- *In the intermediate P_{O_2} region (region 2)*, and near stoichiometric region, the electrical conductivity plots as a function of $\log P_{O_2}$ cross each other. Then $\log\sigma$ is a linear function of $\log P_{O_2}$, with a slope close to 1/2 (Figs. 1 and 2), in agreement with literature data [30,31]. These results can be adequately explained by assuming the presence of (2:2:2)′ defect clusters proposed by Willis [13], as we shall see in Section 4.
- *At higher P_{O_2}, in the vicinity of U_4O_9 (region 3)* and for $T > 1273$ K, the electrical conductivity isotherms are close to each others. In this region the time to reach an equilibrium value was very long, as already observed by Dudney et al. [30]. So these results are less precise than the other results. As we shall see in the following, this sluggish behavior of the material is compatible with the presence of large defect aggregates suggested by different authors [1,4,8–13].

3.2. Chemical diffusion results

After an abrupt change of either P_{O_2} or T, the time to reach an equilibrium electrical conductivity value decreases rapidly as the composition of UO_{2+x} approaches the stoichiometric composition. So, the measurements of $\widetilde{D}$ were performed mainly in region 2 (Fig. 1), where the time to reach an equilibrium value is compatible with the long time approximation (Eq. (3)). As an example, Fig. 3 presents the change of the conductivity during a transient state. Within the experimental errors, the same values of $\widetilde{D}$ were obtained after an abrupt change of either P_{O_2} or T or after an oxidation or reduction reaction, in the same P_{O_2} range. The values obtained for the chemical diffusion coefficient are reported in Fig. 4, for two different ranges of P_{O_2}, i.e. for two different ranges of departure from stoichiometry. They show that $\widetilde{D}$ increases when the defect concentration decreases, while the activation energy does not change significantly. In the high P_{O_2} range, corresponding to a departure from stoichiometry included between $x = 0.07$ and $x = 0.17$, the chemical diffusion coefficient is more that one order of magnitude lower than the values of $\widetilde{D}$ obtained for $x \leqslant 0.03$. In Fig. 5, we have compared our results with those obtained by different authors [1,15–21]. The value of the chemical diffusion activation energy does not change significantly between the results obtained by different authors except those from Bittel [16]. However, our results are generally lower than those of the literature. This discrepancy may be attributed to the various experimental methods and to experiments performed under not well-defined oxygen partial pressures. The data of Lay [17], for instance, were determined from the reduction of $UO_{2.08}$ to $UO_{2.004}$ in a hydrogen stream, without control of P_{O_2}. However, although our results are lower than those obtained by Bayoglu and Lorenzelli [15] (Fig. 5), these authors confirm the same dependence of $\widetilde{D}$ as a function of the departure from stoichiometry (x).

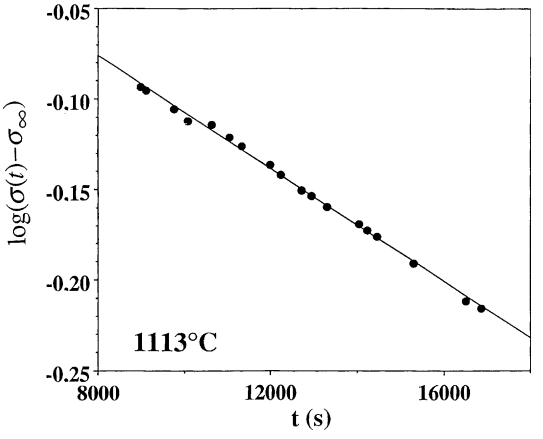

Fig. 3. Electrical conductivity as a function of time after an abrupt change of the oxygen partial pressure from $P_{O_2} = 3.2 \times 10^{-6}$ atm to $P_{O_2} = 3.2 \times 10^{-7}$ atm.

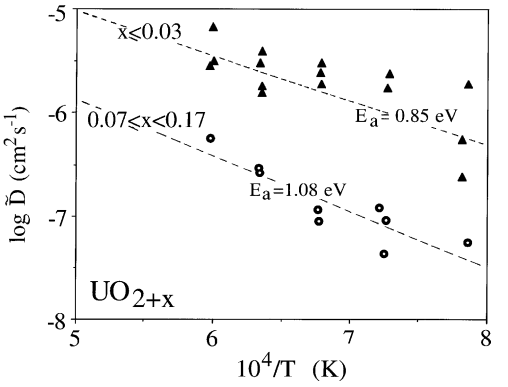

Fig. 4. Chemical diffusion coefficient in UO_{2+x} as a function of the temperature, for different departure from stoichiometry ranges.

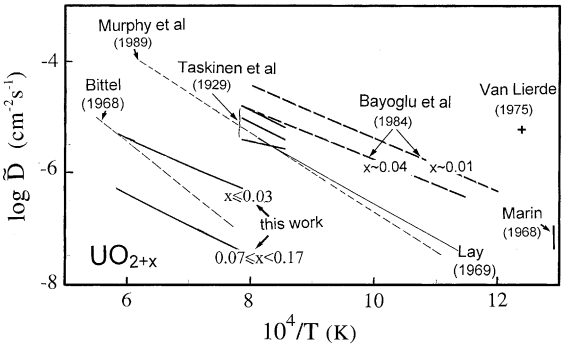

Fig. 5. Chemical diffusion coefficient in UO_{2+x}. Comparison with literature data.

4. Discussion

Our results show the decrease of $\widetilde{D}$ with x, while the oxygen diffusion coefficient values D_O reported in the literature increase with x in the same departure from stoichiometry range ($0 < x < 0.17$). In the following we will first estimate the enthalpy of formation of the (2:2:2)′ Willis clusters evidenced by electrical conductivity measurements. Then we will show that the presence of these clusters allow to show that $\widetilde{D}$ is a decreasing function of the departure from stoichiometry.

4.1. Analysis of the electrical conductivity results

4.1.1. General equations

One can recall first that the formation of the isolated oxygen interstitials can be described, using the Kröger Vink formalism, by the relation [3]:

$$1/2\,O_2 \Longleftrightarrow O_i^{\beta'} + \beta h^{\bullet} \quad K_i = [h^{\bullet}]^{\beta}[O_i^{\beta\prime}]P_{O_2}^{-1/2}. \tag{4}$$

Inserting the electroneutrality condition ($\beta[O_i^{\beta\prime}] = [h^{\bullet}]$) in Eq. (4) and assuming that the electronic defects $h^{\bullet}$ move by a small polaron mechanism thermally activated ($\mu_h = \mu_h^0 \exp(-\frac{\Delta H_m^h}{RT})$), one can show that the p-type conductivity (Eq. (1)) can be expressed by

$$\sigma_p = e\mu_h p = C\mu_h^0 P_{O_2}^{1/2(\beta+1)} \exp\frac{1}{T}\left(-\frac{\Delta H_f}{\beta+1} - \Delta H_m^h\right), \tag{5}$$

where C is a constant, μ_h the mobility of the electron holes $h^{\bullet}$, ΔH_m^h the enthalpy of mobility of one mole of holes assuming a small polaron mechanism thermally activated, p the concentration of holes per cm^3 and ΔH_f the enthalpy of formation of one mole of $O_i^{\beta'}$ (Eq. (4)).

For $T \leqslant 1273$ K and from the extrinsic conductivity values (σ_{ext}) corresponding to the plateaux (Fig. 1), we have found for the activation energy of migration of the electronic defects, assuming a small polaron mechanism thermally activated ($\sigma_{ext} = A \exp\frac{1}{RT}(-\Delta H_m^h)$) : $\Delta H_m^h = 0.17$ eV [23,32].

Remark 2. It should be noted that the extrinsic electrical conductivity results fitted also quite well if one assumes an adiabatic ($\mu_h = \mu_h^0 \frac{1}{T} \exp(-\frac{\Delta H_m^h}{RT})$) or a non-adiabatic small polaron mechanism ($\mu_h = \mu_h^0 \frac{1}{T^{3/2}} \exp(-\frac{\Delta H_m^h}{RT})$). One obtains then $\Delta H_m^h = 0.260$ eV or $\Delta H_m^h = 0.306$ eV, respectively.

In region 2 (Fig. 1), the slope $(\partial \log\sigma/\partial \log P_{O_2})_T$ is close to 1/2 in the linear part of the representations, which corresponds to a departure from stoichiometry lower than $x < 0.1$, according to Hagemark et al. [28]. These electrical conductivity results are consistent with the presence of prevailing $(2O_i^{a'}\ 2O_i^{b'}\ 2V_O^{c\bullet})^{\alpha'}$ Willis clusters [9–13], singly ionized ($\alpha = 1$) and whose formation can be described by

$$2O_O + O_2 \Longleftrightarrow (2O_i^{a'} 2O_i^{b'} 2V_O^{c\bullet})' + h^{\bullet}. \tag{6}$$

From the electroneutrality condition ($[(2O_i^{a'}\ 2O_i^{b'} 2V_O^{c\bullet})'] = [(2:2:2)'] = [h^{\bullet}]$), and assuming that the hole mobility is independent of P_{O_2}, one obtains

$$\sigma_p = e\mu_h p = C_p \mu_h^0 P_{O_2}^{1/2} \exp\frac{1}{RT}\left(-\frac{\Delta H_f}{2} - \Delta H_m^h\right), \tag{7}$$

where ΔH_f is the enthalpy of formation of one mole of cluster and C_p a constant.

4.1.2. Enthalpy of formation of the clusters

In region 2, the electrical conductivity is a decreasing function of T (Fig. 1). Consequently, since the hole mobility is an increasing function of T (Eq. (5), $\Delta H_m^h = 0.17$ eV), the enthalpy of formation of the defects is negative (Eq. (7)). This enthalpy of formation was determined from the linear part of the $\log\sigma = f(\log P_{O_2})$ isotherms, included between 1273 and 1573 K (Fig. 1), and the slope of which is equal to 1/2. From the Arrhenius plots of the conductivity, for different ranges of P_{O_2} (Eq. (5)/ $\Delta H_\sigma = \frac{\Delta H_f}{\alpha+1} + \Delta H_m^h$), we have obtained a mean value for the enthalpy of formation of the defects: $\Delta H_f = -1.7 \pm 0.6$ eV.

This negative value of ΔH_f confirms the existence of strong interactions between defects, in agreement with the presence of defect aggregates, such as the Willis defects $(2{:}2{:}2)'$. One can point out that this result is in good agreement with the value $\Delta H_f = -1.29$ eV calculated by Catlow [33], for a neutral cluster.

Remark 3. One can point out that this value is not significantly modified assuming an adiabatic or a non-adiabatic polaron process (cf. Remark 2).

4.2. Chemical diffusion

In the following, taking into account the experimental results of D_O^* [14], we will show that the presence of clusters can explain the decrease of $\widetilde{D}$ when the departure from stoichiometry increases. Under non-equilibrium conditions, the flux of oxygen ions ($J_{O^{2-}}$) and electrons ($J_{e'}$) in a one dimensional experiment, with respect to the laboratory reference frame and neglecting correlation effects, is given by the following equation [2,3]:

$$J_{O^{2-}} = -\frac{C_O D_O}{RT}\frac{d\eta_{O^{2-}}}{dz} = -\frac{C_O D_O}{RT}\left[\frac{d\mu_{O^{2-}}}{dz} - 2F\frac{d\Phi}{dz}\right], \tag{8}$$

$$J_{e'} = -\frac{C_e D_e}{RT}\left[\frac{d\mu_{e'}}{dz} - F\frac{d\Phi}{dz}\right], \tag{9}$$

where C_i is the concentration of species 'i' (in mol/cm^3), D_i their diffusion coefficient, F the Faraday constant, $d\eta_i/dz$ and $d\mu_i/dz$ the electrochemical and chemical potential gradients, respectively, and $d\Phi/dz$ the Nernst field which appears in the material, due to the difference of mobility of the oxygen defects and of the electronic defects. The Nernst field as well as $d\mu_i/dz$ cannot be determined experimentally. These terms are eliminated from the flux equations (Eqs. (8) and (9)) by means of the coupling condition between the electronic defects and the oxygen ions [3,5,6,34]:

$$\Sigma z_i J_i = 0, \tag{10}$$

where z_i is the electrical charge of the species i.

From Eqs. (8) and (9), it follows:

$$F\frac{\mathrm{d}\Phi}{\mathrm{d}z}=\frac{2C_{\mathrm{O}}D_{\mathrm{O}}\frac{\mathrm{d}\mu_{\mathrm{O}^{2-}}}{\mathrm{d}z}+C_{\mathrm{e}}D_{\mathrm{e}}\frac{\mathrm{d}\mu_{\mathrm{e}}}{\mathrm{d}z}}{4C_{\mathrm{O}}D_{\mathrm{O}}+C_{\mathrm{e}}D_{\mathrm{e}}}. \tag{11}$$

Taking into account Eq. (11) and the local equilibrium condition: $\mathrm{O}^{2-}\Longleftrightarrow \mathrm{O}+2\mathrm{e}'$ (i.e. $\mathrm{d}\mu_{\mathrm{O}^{2-}}=\mathrm{d}\mu_{\mathrm{O}}+2\mathrm{d}\mu_{\mathrm{e}}$,), Eq. (8) can be written in the case of a semiconducting compound, ($C_{\mathrm{O}}D_{\mathrm{O}}\ll C_{\mathrm{e}}D_{\mathrm{e}}$):

$$J_{\mathrm{O}^{2-}}=-\frac{C_{\mathrm{O}}D_{\mathrm{O}}}{RT}\frac{\mathrm{d}\mu_{\mathrm{O}}}{\mathrm{d}z}=-\frac{C_{\mathrm{O}}D_{\mathrm{O}}}{2}\nabla\ln P_{\mathrm{O}_2}. \tag{12}$$

On the other hand, if one assumes that the transport processes are controlled by the flux of (2:2:2)′ Willis clusters (cl), Eq. (2) can be written:

$$J_{\mathrm{O}^{2-}}=2J_{\mathrm{cl}}=-2\widetilde{D}\nabla C_{\mathrm{cl}}. \tag{13}$$

From Eqs. (12) and (13), one obtains:

$$\widetilde{D}=\frac{C_{\mathrm{O}}D_{\mathrm{O}}}{4C_{\mathrm{cl}}}\frac{\mathrm{d}\ln P_{\mathrm{O}_2}}{\mathrm{d}\ln C_{\mathrm{cl}}}. \tag{14}$$

At constant temperature and according to the equilibrium constant of Eq. (6) ($K_{\mathrm{cl}}=x_{\mathrm{cl}}^2/P_{\mathrm{O}_2}$, where x_{cl} represents the cluster molar fraction), one obtains:

$$2\mathrm{d}\ln x_{\mathrm{cl}}=\mathrm{d}\ln P_{\mathrm{O}_2}. \tag{15}$$

Furthermore, it follows from Eq. (A.2) (cf. Appendix A) that:

$$\frac{C_{\mathrm{O}}}{C_{\mathrm{cl}}}=\frac{x_{\mathrm{O}}}{x_{\mathrm{cl}}}=2\frac{2+x}{x}, \tag{16}$$

where x_{O} represents the molar fraction of oxygen.

Inserting Eqs. (15) and (16) in Eq. (14), and assuming that $\frac{x_{\mathrm{O}}}{C_{\mathrm{O}}}\approx\frac{\mathrm{d}x_{\mathrm{cl}}}{\mathrm{d}C_{\mathrm{cl}}}$, yields:

$$\widetilde{D}=\frac{x_{\mathrm{O}}D_{\mathrm{O}}}{2x_{\mathrm{cl}}}=D_{\mathrm{O}}\frac{2+x}{x}. \tag{17}$$

In order to compare our experimental results of $\widetilde{D}$, obtained in the temperature range 1000–1400 °C, to the values of $\widetilde{D}$ calculated from Eq. (17), we have extrapolated at 1000 °C the results of D_{O}^{*} obtained by Contamin et al. [14], at $T\leqslant 900$ °C. Since there are not experiments for throwing light on diffusion mechanism in UO_{2+x}, we have assumed, as proposed in the literature [12], that the transport of oxygen occurs by the interstitial mechanism or something similar. Therefore, we have assumed [2] that the jumps of the ions are not correlated ($D_{\mathrm{O}}^{*}\approx D_{\mathrm{O}}$). The fit of the experimental results of Contamin et al. [14], extrapolated at 1000 °C, is then given by

$$\log D_{\mathrm{O}}=(-7.9+6x), \tag{18}$$

where D_{O} is expressed in $\mathrm{cm}^2\,\mathrm{s}^{-1}$.

Inserting Eq. (18) in Eq. (17), yields

$$\log\widetilde{D}=-7.9+6x+\log(2+x)-\log x. \tag{19}$$

From Eq. (19), one obtains:

$$\frac{\mathrm{d}\log\widetilde{D}}{\mathrm{d}x}=\frac{1}{2.3}\frac{13.8x^2+27.6x-2}{x(2+x)}. \tag{20}$$

When $x<0.07$ (limit positive value which annuls the numerator of Eq. (20)), it follows from Eq. (20) that $\frac{\mathrm{d}\log D}{\mathrm{d}x}<0$. Consequently, the values of $\widetilde{D}$ calculated from the results of D_{O} (Eq. (20)) decrease when the departure from stoichiometry x increases in the range $0<x<0.07$, in agreement with our experimental results (Fig. 4).

Remark 4. In our calculations we have assumed that the prevailing defects are the Willis clusters (2:2:2)′, singly ionised, which prevail when $x<0.1$ (cf. Section 4.1). The departure from stoichiometry $x=0.07$ corresponds then to their upper prevailing influence limit. However, $\widetilde{D}$ continues to decrease when $x\geqslant 0.07$ (cf. Sections 3.1 and 3.2). This can be explained by Willis defects α time ionized or by more complex defect aggregates.

One can point out that the decrease of $\widetilde{D}$, when the departure from stoichiometry increases, can also be explained by a reduction of the defect mobility due to transport processes occurring via a dynamic exchange between mobile small defects and defects temporarily immobilized in larger clusters or domains, as suggested in the literature [4,10–12].

Table 2 shows the good agreement between our experimental results of $\widetilde{D}$ and the calculated values, using Eq. (17). At $T>1000$ °C, the calculations have been performed using the values of D_{O} deduced from Eq. (18) and according to the activation energy of diffusion (~0.93 eV) proposed by Contamin et al. [14]. It

Table 2
Experimental and calculated chemical diffusion coefficient values in the stoichiometric range of validity of the proposed model (Eq. (17))

Temperature (°C)	P_{O_2} (atm)	x	$\widetilde{D}_{\mathrm{exp}}$ ($\mathrm{cm}^2\,\mathrm{s}^{-1}$)	$\widetilde{D}_{\mathrm{cal}}$ ($\mathrm{cm}^2\,\mathrm{s}^{-1}$)	$\widetilde{D}_{\mathrm{cal}}/\widetilde{D}_{\mathrm{exp}}$
1000	1.58×10^{-10}	0.013	2.4×10^{-7}	2.3×10^{-6}	≈9.6
1300	6.45×10^{-9}	0.008	3.9×10^{-6}	1.7×10^{-5}	≈4.4
1400	2.69×10^{-7}	0.030	2.8×10^{-6}	9.6×10^{-9}	≈3.4

should be noted that $\widetilde{D}$ was calculated in the validity range of Eq. (18) and for $x \leqslant 0.07$ (cf. Eq. (20)).

5. Conclusion

In this work, electrical conductivity measurements have been performed in thermodynamic and non-equilibrium conditions as a function of P_{O_2} and T. In the intermediate P_{O_2} range ($10^{-8} < P_{O_2} < 10^{-11}$ atm), the equilibrium conductivity results suggest the prevailing influence of the (2:2:2)′ Willis clusters. We have found for the enthalpy of formation of these defects $\Delta H_f = -1.7 \pm 0.6$ eV. At higher P_{O_2}, at the vicinity of U_4O_9, we have found that the time to reach an equilibrium electrical conductivity value becomes increasingly sluggish. This is consistent with the presence either of large defect aggregates or defects arranged in domains. On the other hand, electrical conductivity measurements performed in transient state have allowed us to determine the chemical diffusion coefficient. We have shown that $\widetilde{D}$ is a decreasing function of the departure from stoichiometry in the range $0 < x < 0.17$, while the activation energy does not change significantly. For $x < 0.07$, a formal analysis of the transport processes under non-equilibrium conditions has allowed us to show that the changes of $\widetilde{D}$ with x are consistent with those of the oxygen self-diffusion coefficient (D_O^*) in the P_{O_2} and temperature range of stability of the clusters [2:2:2]′. For $x \geqslant 0.7$, the decrease of $\widetilde{D}$ when x increases can be explained either by Willis defects α time ionized or by more complex defect aggregates or via a dynamic exchange between mobile small defects and defects temporarily immobilized in larger clusters or domains.

Appendix A. Expression of $\frac{x_O}{x_{cl}}$ as a function of the departure from stoichiometry

Let us consider that the (2:2:2)′ Willis clusters are the prevailing defects, as suggested by the experimental results [23,32]. If $n_{O_{st}}$ and n_U are the oxygen and uranium ion numbers per cm^3 for the stoichiometric composition, we can write $\frac{n_{O_{st}}}{n_U} = 2$ and for the non-stoichiometric composition $\frac{n_O}{n_U} = 2 + x$. It should be noted that the (2:2:2)′ cluster contains 2 oxygen vacancies and 4 oxygen interstitials ($(2O_i^{a'}\ 2O_i^{b'}\ 2V_O^{c^{\cdot}})'$), with two oxygen interstitials arising from the oxygen sublattice (Eq. (6)). If n_{cl} is the number of clusters per cm^3, this yields:

$$n_O = n_O \text{ (on the oxygen sublattice)} + 4n_{cl}$$
$$\text{with } n_O \text{ (on the oxygen sublattice)} = n_{O_{st}} - 2n_{cl}.$$

$$\text{Therefore, } n_O = 2(n_U + n_{cl}). \tag{A.1}$$

If one expresses the molar fractions: $x_{cl} = \frac{\frac{n_O}{2} - n_U}{2n_U + 5n_{cl}}$ and $x_O = \frac{(2+x)n_U}{2n_U + 5n_{cl}}$, one obtains finally

$$\frac{x_O}{x_{cl}} = \frac{2(2+x)}{x}, \tag{A.2}$$

where $2n_U + 5n_{cl}$ is the sum of oxygen ion, oxygen vacancy and cluster numbers per cm^3.

References

[1] V. Haase, L. Manes, B. Schultz, G. Schumacher, D. Vollath, in: R. Keim, C. Keller (Eds.), Uranium, Gmelin Handbook of Inorganic Chemistry, Supplement Volume C4, Springer-Verlag, Berlin, 1986.
[2] J. Philibert, Atom Movements, Diffusion and Mass Transport in Solids, Editions de Physique, 1991.
[3] F.A. Kröger, Chemistry of Imperfect Crystals, North Holland Publishing Company, Amsterdam, 1964.
[4] H. Matzke, in: T.O. Sorensen (Ed.), Nonstoichiometric Oxides, Materials Science Series, Academic Press, 1981, p. 155.
[5] G. Petot-Ervas, C. Petot, D. Monceau, G. Sproule, M. Graham, J. Am. Ceram. Soc. 78 (1995) 2314.
[6] G. Petot-Ervas, C. Petot, J. Phys. Chem. Solids 51 (1990) 901.
[7] D. Korfiatis, S. Potamianou, E. Tsagarakis, K. Thoma, Solid State Ionics 136&137 (2000) 1367.
[8] C.R.A. Catlow, A.B. Lidiard, in: Thermodynamics of Nuclear Fuels, vol. 2, IAEA, Vienna, 1974, p. 27.
[9] C.R.A. Catlow, in: T.O. Sorensen (Ed.), Nonstoichiometric Oxides, Materials Science Series, Academic Press, 1981, p. 61.
[10] G.E. Murch, Diffus. Defects Data 32 (1983) 9.
[11] G.E. Murch, C.R.A. Catlow, in: F.J. Kedven, D.L. Beke (Eds.), Diffusion in Metals and Alloys, Institute for Applied Physics, Debrecen, Hungary, 1983, p. 9.
[12] G.E. Murch, C.R.A. Catlow, J. Chem. Soc. Faraday Trans. 2 (1987) 1157.
[13] B. Willis, Acta Crystallogr. 18 (1965) 75.
[14] P. Contamin, J.J. Bacmann, J.F. Marin, J. Nucl. Mater. 42 (1972) 54.
[15] A.S. Bayoglu, R. Lorenzelli, Solid State Ionics 12 (1984) 53.
[16] J.T. Bittel, J. Am. Ceram. Soc. 52 (1968) 8.
[17] K.W. Lay, J. Am. Ceram. Soc. 30 (1969) 16.
[18] J.F. Marin, Report CEA-Nu883, 1968.
[19] W. Van Lierde, unpublished results;
Cited by G.E. Murch, Philos. Mag., 32 (6) (1975) 1120.
[20] J. Murphy, K.S. Norwood, Report UKAEA Harwell Laboratory, 1989.
[21] A. Taskinen, H. Kullberg, J. Nucl. Mater. 83 (2) (1929) 333.
[22] J. Maluenda, R. Farhi, G. Petot-Ervas, J. Phys. Chem. Solids 10 (1981) 911.
[23] P. Ruello, G. Petot-Ervas, C. Petot, L. Desgranges, J. Am. Ceram. Soc., in press.
[24] W. Jost, Diffusion in Solids, Liquid, Gases, Academic Press, 1960.

[25] J.B. Price, J.B. Wagner, Z. Phys. Chem. Neue Fol. 49 (1966) 257.
[26] T.L. Markin, V.J. Wheeler, R.J. Bones, J. Inorg. Nucl. Chem. 30 (1968) 807.
[27] Y. Saito, J. Nucl. Mater. 51 (1974) 112.
[28] K. Hagemark, M. Brogli, J. Inorg. Nucl. Chem. 28 (1966) 2837.
[29] B. Touzelin, M. Dodé, Rev. Int. Hautes Temp. Refract. 6 (1969) 267.
[30] N.J. Dudney, R.L. Coble, H.L. Tuller, J. Am. Ceram. Soc. 64 (11) (1981) 627.
[31] S.H. Kang, J.H. Lee, H.I. Yoo, H.S. Kim, Y.W. Lee, J. Nucl. Mater. 277 (2000) 339.
[32] P. Ruello, Phd thesis, Ecole Centrale Paris, 2001.
[33] C.R.A. Catlow, Proc. Royal Soc. London A 353 (1977) 533.
[34] C. Wagner, Atom Movements, American Society for Metals, Cleveland, 1951.